The size dependence of the high-pressure phase stability of II-VI semiconductor nanocrystals

1995 J. Phys.: Condens. Matter 7 8519

(http://iopscience.iop.org/0953-8984/7/45/007)

J. Phys.: Condens. Matter 7 (1995) 8519–8527. Printed in the UK

The size dependence of the high-pressure phase stability of II–VI semiconductor nanocrystals

Markus R Silvestri and John Schroeder

Department of Physics and Center of Glass Science and Technology, Rensselaer Polytechnic Institute, Troy, NY 12180-3590, USA

Received 2 June 1995

Abstract. We report pressure-dependent optical studies for different sized CdS_xSe_{1-x} nanocrystals embedded in a glass matrix. The increase in the phase stability in going from wurtzite to rock salt structure is reversible and size dependent. Different possible sources such as strain from defects, semiconductor-to-glass-matrix thermal expansion mismatch, increase in the electronic energy due to confinement, and surface tension which may cause this effect are discussed. Results indicate that surface tension is the major contribution and a simple model is developed that produces estimates of the size distribution and difference between the surface tensions of the two phases.

1. Introduction

Numerous studies have established the occurrence of changes in the thermodynamic properties of II–VI semiconductor nanocrystals such as the reduction of the melting temperature [1, 2] or an increase in the structural phase transition pressure point [3–9]. This is a novel phenomenon: the stability of nanocrystals can be controlled by an external parameter such as the size. Tolbert *et al* [3, 4] conducted a series of studies on nearly monodisperse CdSe nanocrystals in a colloidal suspension and confirmed a size dependence which was attributed to surface tension. However, similar size dependence studies have not been performed on nanocrystals embedded in a solid glass matrix, which is a composite that has promising potential for technical applications [10]. Diffusion-grown nanocrystals in a glass matrix pose, in many ways, a different problem with respect to phase stability. Strains, a broad size distribution, and a low concentration of the nanocrystals complicate the picture.

It is the goal of this paper to examine these effects in more detail. Also, the question of whether strains originating from defects are important is directly approached by artificially inducing defects in nanocrystals by bombarding the samples with electrons. A very simplified model is applied resulting in a two-parameter fitting function where one of the parameters is the extent of the size distribution, which is a very difficult value to obtain otherwise.

2. Experiment

As samples we used Schott filters RG630 and OG570. These filters are composite materials based on a borosilicate glass containing CdS_xSe_{1-x} crystallites. Their compositions were

0953-8984/95/458519+09$19.50

determined through the relative shift between the S-like and Se-like peak positions in the Raman spectra [11], and their sizes by TEM [12] or x- ray diffraction through the Debye–Scherrer broadening. The composition of RG630 and samples grown from its melt [12] is $CdS_{0.44}Se_{0.56}$ and their sizes are given in the legend of figure 3. Unfortunately, the average size of the nanocrystals in sample C2 could not be resolved by our TEM set-up; nevertheless, according to the blue shift in its optical spectrum, its average size must be distinctively smaller than the average size of the nanocrystals in all other samples. A very rough estimate using the blue shift would set the size near 2 nm. The composition of OG570 is $CdS_{0.7}Se_{0.3}$ and its average size is approximately 7 nm.

For the pressure measurements the samples were polished down to about 40–80 μm thickness and then loaded into a diamond anvil pressure cell, which is described in detail elsewhere [7]. A 4:1 methanol–ethanol mixture served as a pressure medium. The pressures were measured with the standard ruby fluorescence technique. The shape of the ruby lines and their spacing did not alter, indicating that hydrostatic pressure was well maintained throughout all our experiments.

All optical experiments were carried out at 135° scattering geometry at room temperature unless otherwise noted. This set-up has the advantage of a higher collection efficiency and a better signal-to-noise ratio compared to the 180° backward-scattering geometry. In addition we had the option of defocusing the incoming light, if necessary, to keep the power densities low.

Depending on the sample used, the 457.9 nm, 488.0 nm, or 514.5 nm lines of the Ar^+ laser were applied. The photoluminescence spectra were recorded with a Spex double monochromator with slits set to a resolution of about 2 cm^{-1}. A cooled RCA 31034A photomultiplier served as a detector from which the counts were stored in a computer for further processing.

The samples that were irradiated before the optical experiments were bombarded with 10 MeV electrons to induce defects. While water cooled, they were irradiated for approximately two hours at a current of 120 μA.

3. Results and discussion

A typical photoluminescence spectra of sample C6 grown from the melt of RG630 is shown in figure 1. The strong band-edge luminescence peaks in the energy range of 2.0–2.2 eV are clearly visible at pressures far beyond the bulk structural phase transition pressure point (~30 kbar at room temperature). In CdS the high-pressure rock salt phase has an indirect band gap of about 1.5 eV and a similar reduction is also expected for CdSe; thus, the band-edge luminescence at high pressures clearly indicates that nanocrystals remain in the low-pressure wurtzite structure. This experimental observation is further supported by the Raman spectra: Raman lines typical for the wurtzite structure persist up to the same high pressures. However, for quantitative estimates, the Raman lines are difficult to interpret since they are also subject to resonance effects [13]. Also, at high pressures, broad featureless peaks of a deep-level defect are visible. At room temperature they are not easy to make out but nevertheless are present and are more distinct at liquid nitrogen temperatures (see subsection 2, figure 4).

In figure 2 the energy positions of the band-edge and deep-level defect peaks for C6 are plotted as a function of pressure. The different energy shift of the deep-level defect with respect to the band edge indicates that the defect is situated closer to the conduction band edge than the valence band edge.

The filled symbols in figure 2 represent measurements returning from high pressure.

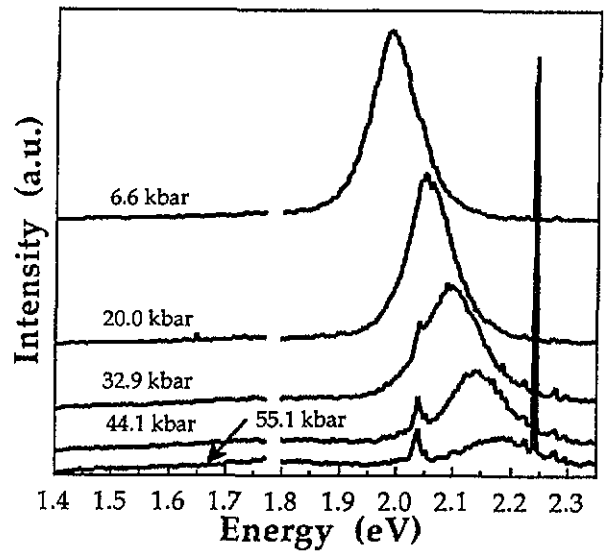

Figure 1. Typical photoluminescence spectra of sample C6 at different pressures at room temperature. The spike around around 2.25 eV is due to the diamond anvils and the emerging peak at around 2.05 eV is from the pressure-transmitting medium. The gap is where the strong ruby lines were bypassed. Note the emergence of a broad deep-level defect at high pressures.

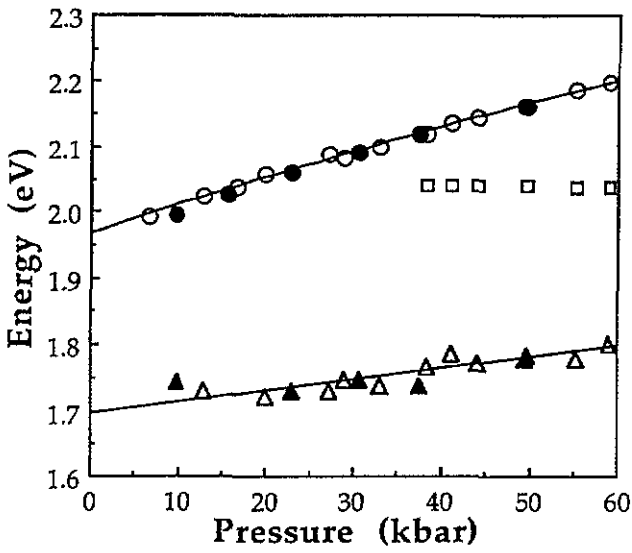

Figure 2. The pressure dependence of the energy positions of the band-edge and defect luminescence peaks of C6. The open squares are the peaks from the pressure medium. Open figures represent increasing pressure and filled figures decreasing pressure.

There is no hysteresis or shifts in position from the initial atmospheric pressure point. Neither was any significant hysteresis or shifts in the Raman spectra detected, in contrast to 30 nm crystallites [14] and the bulk material [15]. When bulk material is cycled through a phase transition, it breaks up into many small crystallites which in turn cause local strains; hence the changes. Venkateswaren *et al* [16] observed that bulk GaAs and AlAs films break

up into 6.5 and 17.5 nm sized crystallites with corresponding shifts in the Raman spectra after cycling through a high-pressure phase. Assuming that similar critical sizes exist for our composites, the results here indicate that the crystallites apparently do not break up into smaller pieces.

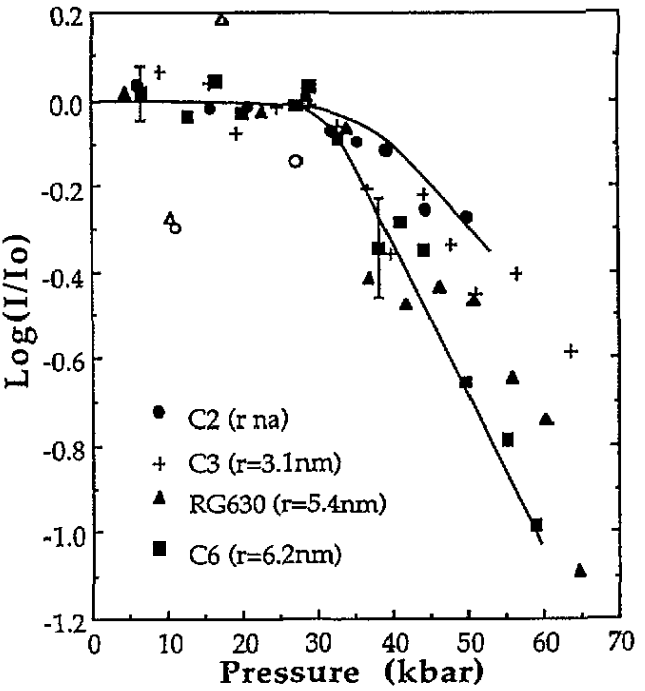

Figure 3. The phase stability for nanocrystals of different average sizes. The luminescence intensities were normalized to the average intensities below 30 kbar. Open figures were considered as outliers. The lines are only guides for the eye, to enable the observer to appreciate the change in phase stability.

The relative intensities of the band-edge luminescence for nanocrystals of four different average sizes are given in figure 3. In order to compare the different samples, the intensities were normalized to the average intensity of measurements that were taken below the bulk phase transition pressure point. Even though the scatter of data is large, an increased phase stability with decreasing size is observable. A number of effects may account for this phenomenon. The most important are: effects from the glass matrix, strains from defects, changes in the electronic energy due to confinement, and surface tension. Each of these effects are discussed and evaluated separately below.

3.1. Effects from the glass matrix

Two principal arguments may be brought up here: firstly, that the nanocrystals are not fully exposed to the pressure since part of it is taken up by the glass matrix and, secondly, that strain may be present due to the thermal mismatch between the CdS_xSe_{1-x} and the glass.

In answer to the first problem, it can be shown [17] that glasses at high pressures behave as an elastic medium and transmit the pressure within a fraction of the time that is taken to measure the external pressures in the diamond anvil cell. Also, high-pressure phase stability is observed in colloidal nanocrystals where no glass matrix is present [7, 18].

The strain caused by thermal mismatch is very small. The glass contracts faster than the nanocrystals while cooling down from the growing temperature (≈900 K), which results in a positive pressure. Taking typical values of 1.07×10^{-5} K^{-1} and 40 GPa for the linear thermal expansion coefficient and bulk modulus for glass and the polynomial coefficients for the thermal expansion for CdS [19], an estimate produces at most a few kilobars and may be neglected in a first approximation.

3.2. Strain from defects

Defects are disorders in the crystal structure causing some local rearrangement of the neighbouring atoms and may therefore induce strain. Luminescence spectra (figures 1 and 4) indicate that at least radiative defects are present [20]. Intuitively, one may then expect that the induced strain must first be overcome in the structural phase transition and, as a consequence, the transition pressure should rise.

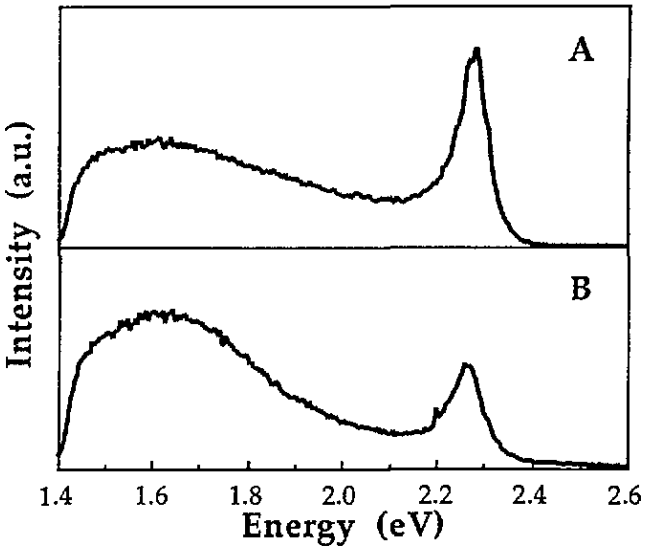

Figure 4. The uncorrected (for spectral response of detection system) luminescence spectra of treated samples of OG570 at liquid N_2 temperatures. A is before and B after electron irradiation.

An effective way to test this idea experimentally is to change the defect concentration in the nanocrystals by irradiating them with energetic electrons. Figure 4 shows the photoluminescence spectra before (A) and after (B) electron bombardment for $CdS_{0.7}Se_{0.3}$ nanocrystals (sample OG570). Not only a change in the ratio of defect to band-edge peak intensities occurred, but also the absolute intensities of the defects increased strongly suggesting that there are more radiative defects in the irradiated samples than in the original samples. Even taking the spectral response of the detection system into account does not alter this observation. However, these changes had no large-scale effect on the phase stability as figure 5 illustrates.

The fact that defects are unlikely to be important in the phase stability arises from the fact that this phase transition is reconstructive (i.e. bonds are broken), requiring a lot of energy as the following numerical example will demonstrate. Since the bulk modulus for CdS is 60.7 GPa and its first pressure derivative 0.42, the Murnighan equation [21], which relates the volume to the pressure, may be linearized; thus the change in the Gibbs

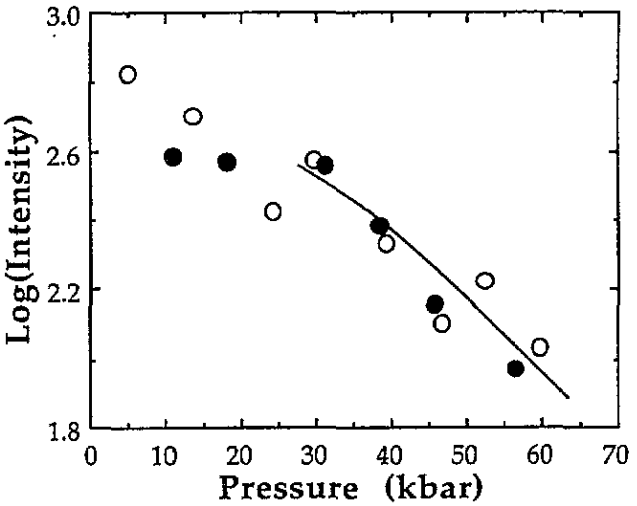

Figure 5. Photoluminescence intensities as a function of pressure of samples A and B of OG570. The open circles represent A and the filled circles B. Again, the line is a guide for the eye.

free energy ΔG can be readily computed from $-\int P\,dV$ and is about 2 kJ mol^{-1}. For nanocrystals of a radius of 4 nm this is equivalent to an energy of about 108 eV. Under similar approximations used for the lattice energy of III–V semiconductors in the studies of Singh and Singh [22], $\Delta G(P)$ may be, as a first approximation, linearized since the changes in the interatomic distances are small. In other words, an increase of 20 kbar in the phase transition pressure point corresponds to an energy change of about 72 eV. Because of the small number of Cd–S atom pairs in the nanocrystal in this example, a few defects inside the crystal would already constitute a high defect concentration; consequently, each defect would have to account for a much too large an energy.

3.3. Confinement

Due to the small sizes of the crystallites, the conduction and valence bands transform into a series of discrete states. This results in an increase of the electronic energy and is also observed optically as a blue shift. Since at the phase transition point the volume of the crystallites collapses by about 20%, this quantum confinement effect will be further enhanced and, in principle, if the energy increase is large enough, the phase transition pressure point could be shifted to higher pressures.

In the case of very strong confinement, where the leading term of the asymptotic formula of the confinement energy [23] is good enough for a rough estimate, the change in electronic energy is

$$\Delta E = \frac{\hbar^2\pi^2}{2\mu R^2}\left(\frac{1}{f} - 1\right) \tag{1}$$

where R is the radius of the nanocrystal, μ the effective reduced mass, and $f = 0.86$ taking the volume collapse into account. Applying typical numbers for CdS or CdSe to equation (1) produces, even for small radii, energy changes that are far too small. As a consequence, to produce the desired change in the phase stability, carrier densities rather typical of metals are necessary.

3.4. Surface tension

Crystallites in the nanosize regime have a large number of atoms within the surface area. Consequently, the surface energy must contribute substantially to the total energy of the crystallite. Since in solids the temperature dependence of the surface tension is very small, the surface tension is nearly equal to the surface energy and therefore this will be used below.

If the surface tension in the rock salt phase is larger than that in the wurtzite phase, an additional energy must be overcome in the phase transition resulting in an increase in the phase transition pressure point. Intuitively, higher surface tension in the rock salt phase is plausible since the rock salt structure has a higher coordination number than the wurtzite structure. Therefore, a surface atom in the rock salt phase maintains, on average, more bonds, i.e. it will have a stronger inward attraction or potential energy.

Using the same justification as in subsection 3.2, the difference in the Gibbs free energy ΔG is linearized in pressure. Including the surface tension γ_i, ΔG at temperature $T = 0$ is

$$\Delta G = a(P_0 - P) + 4\pi R_W^2 (f'\gamma_R - \gamma_W). \tag{2}$$

The subscripts R and W stand for rock salt and wurtzite, R_i for the radii of the nanoparticles and $f' = R_R^2/R_W^2$. The condition for phase transition is $\Delta G = 0$. The normalized enhancement of the phase transition then reads

$$\frac{\Delta P}{P_0} = C_S \frac{R_0}{R_W} \tag{3a}$$

$$C_S = \frac{3(f'\gamma_R - \gamma_W)}{a_0 P_0 R_0} \tag{3b}$$

where P_0 is the bulk phase transition pressure point and a_0 is 'a' normalized to the particle volume. R_0 is the average particle radius and was introduced for convenience to keep C_S and parameters A and B below unitless. Assuming a Gaussian size distribution, the relative number of particles resisting a phase transition is

$$n = C_N \int_{R_{min}}^{R_t} e^{(R-R_0)^2/2\sigma^2}\, dR \approx \frac{1}{\sqrt{2\pi}\sigma} \int_{-\infty}^{R_t} e^{(R-R_0)^2/2\sigma^2}\, dR \tag{4}$$

and assuming that the relative luminescence intensity is proportional to the number of particles in the wurtzite phase, equation (4) becomes

$$\log\left(\frac{I}{I_0}\right) = \log\left\{\frac{1}{2}\left[1 + \operatorname{erf}\left(\frac{A}{x} - B\right)\right]\right\} \tag{5}$$

where $x = \Delta P/P_0$, $A = C_S B$, and $B = R_0/(\sqrt{2}\sigma)$. From fitting this two-parameter function one obtains the dispersion of the size distribution and $\Delta\gamma'$ $(= f\gamma_R - \gamma_W)$. An example of such a fit is given in figure 6. The r^2 and F values are 0.92 and 68. The parameters of the fits for all four samples are given in table 1.

The fits are not very good which may be in part blamed on the large uncertainty, scatter, small number of data points, and simplicity of the model. Nevertheless, the numbers in table 1 are encouraging and indicate that surface tension is in fact the dominant factor in the phase stability of nanocrystals embedded in glass. The increase in size dispersion with decreasing size is also confirmed by broader peaks in the optical spectra and is consistent with the expectations of the growth mechanism in these glasses; however, the values seem somewhat on the large side. The values of $\Delta\gamma'$ in column five seem to be reasonable if they are compared with typical values for γ of solids, though they could not be confirmed since γ values for both phases for our compounds are not available.

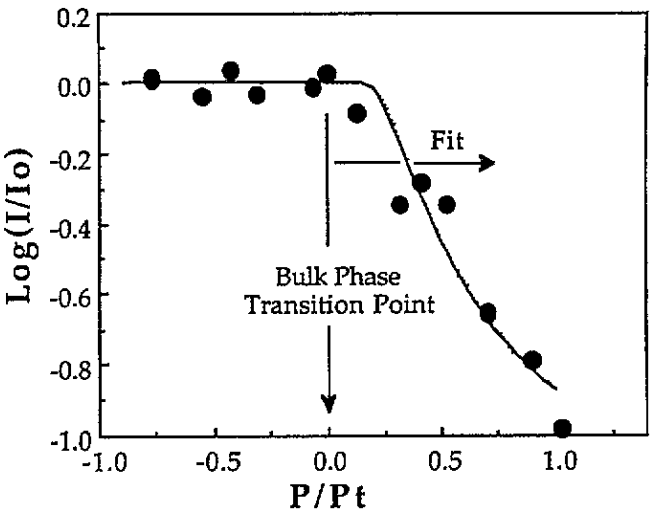

Figure 6. The fitted line shape function of the relative luminescence intensities of sample C6.

Table 1. Size dispersion and surface tensions.

Sample	R_0 (nm)	C_S	σ/R_0	$\Delta\gamma'$ (N m^{-1})
C2	N.A.	(1.01 ± 1.46)	(3.9 ± 3.9)	—
C3	3.1	0.41 ± 0.22	(1.5 ± 0.4)	0.029 ± 0.016
RG630	5.4	0.43 ± 0.25	0.58 ± 0.12	0.053 ± 0.031
C6	6.2	0.41 ± 0.13	0.53 ± 0.06	0.058 ± 0.018

4. Summary and conclusion

From photoluminescence measurements we found that the structural phase transition induced by pressure in nanocrystalline systems is quite different from that in bulk materials. The phase transition in bulk materials is sharp [15] but for nanocrystals it is broad and occurs at higher pressures. A size study of the phase stability was conducted and a correlation between size and increase in the phase stability was established.

Several possible sources causing this effect were examined. Of the four principal sources (glass matrix, defects, confinement, and surface tension), it was found that three of them are unlikely because they contribute energetically too little to the total free energy of the nanocrystallites. One of them, defects, was also experimentally tested and confirmed the predictions of the theoretical considerations.

For the remaining possible cause, surface tension, a simple model was applied from which a two-parameter fitting function was developed. The values for the fitting parameters (size dispersion σ and $\Delta\gamma'$) were of reasonable magnitude and also confirmed some tendencies observed in the optical spectra indicating that the idea of surface tension is correct. However, for reliable quantitative results more refined models are required.

Acknowledgments

The authors gratefully acknowledge the support of this work by the National Science Foundation under Grant No DMR-88-01004. They also would like to thank Guang Mei for providing the data of the average particle sizes for the sample series C2, C3, RG630 and C6.

References

[1] Goldstein A N, Echer C M and Alivisatos A P 1992 *Science* **256** 1425
[2] Buffat P and Borel J P 1976 *Phys. Rev.* A **13** 2287
[3] Tolbert S H and Alivisatos A P 1994 *Science* **265** 373
[4] Tolbert S H, Herhold A B, Johnson C S and Alivisatos A P 1994 *Phys. Rev. Lett.* **73** 3266
[5] Alivisatos A P, Harris T D, Brus L E and Jayaraman A 1988 *J. Chem. Phys.* **89** 5979
[6] Haase M and Alivisatos A P 1992 *J. Phys. Chem.* **96** 6756
[7] Zhao X S, Schroeder J, Persans P D and Bilodeau T G 1991 *Phys. Rev.* B **43** 12 580
[8] Zhao X S, Schroeder J, Silvestri M R, Bilodeau T G and Persans P D 1991 *Clusters and Cluster Assembled Materials (MRS Symp. Proc. 206)* ed R S Averback, J Bernholc and D L Nelson (Pittsburgh, PA: Materials Research Society) p 151
[9] Schroeder J *et al* 1990 *Chemical Processes in Inorganic Materials: Metal and Semiconductor Clusters and Colloids (MRS Symp. Proc. 272)* ed P D Persans, J S Bradley, R R Chianelli and G Schmid (Pittsburgh, PA: Materials Research Society) p 251
[10] Lawendy N M and MacDonald R L 1991 *J. Opt. Soc. Am.* B **8** 1307
[11] Persans P D *et al* 1990 *Materials Issues in Microcrystalline Semiconductors (MRS Symp. Proc. 164)* ed P M Fauchet, K Tenaka and C C Tsai (Pittsburgh, PA: Materials Research Society) p 105
[12] Mei G, Carpenter S, Felton L E and Persans P D 1992 *J. Opt. Soc. Am.* B **9** 1394
[13] Silvestri M R and Schroeder J 1994 *Phys. Rev.* B **50** 15 108
[14] Variano B F, Schlotter N E, Hwang D M and Sandroff C J 1988 *J. Chem. Phys.* **88** 2848
[15] Zhao X S, Schroeder J, Bilodeau T G and Hwa L G 1989 *Phys. Rev.* B **40** 1257
[16] Venkateswaren U D, Cui L J and Weinstein B A 1992 *Phys. Rev.* B **45** 9237
[17] Schroeder J 1977 *Treatise on Materials Science and Technology* vol 12 *Glass I: Interaction with Electromagnetic Radiation* (New York: Academic) p 157
[18] Hwang L W, Schroeder J, Silvestri M R and Zhao X S 1994 *High-Pressure Science and Technology (AIP Conf. Proc. 309)* ed S C Schmidt, J W Shaner, G A Samara and M Ross (New York: American Institute of Physics) p 605
[19] Touloukian Y S (ed) 1977 *Thermal Expansion of Nonmetallic Solids* vol 13 (New York: IFI/Plenum) p 1221
[20] Bebb H B and Williams E W 1972 *Semiconductors and Semimetals: Transport and Optical Phenomena* vol 8, ed R K Willardson and A C Beer (New York: Academic) p 181
[21] Murnaghan F D 1944 *Proc. Natl Acad. Sci. USA* **30** 244
[22] Singh R K and Singh S 1989 *Phys. Rev.* B **39** 671
[23] Kayanuma Y and Momiji H 1990 *Phys. Rev.* B **41** 10 261